Accepted Manuscript

Towards online Near-Infrared spectroscopy to optimise food product mixing

Angela Barone, Jarka Glassey, Gary Montague

PII: S0260-8774(19)30274-2

DOI: https://doi.org/10.1016/j.jfoodeng.2019.07.003

Reference: JFOE 9656

To appear in: *Journal of Food Engineering*

Received Date: 29 August 2018

Revised Date: 3 July 2019

Accepted Date: 4 July 2019

Please cite this article as: Barone, A., Glassey, J., Montague, G., Towards online Near-Infrared spectroscopy to optimise food product mixing, *Journal of Food Engineering* (2019), doi: https://doi.org/10.1016/j.jfoodeng.2019.07.003.

Towards Online Near-Infrared Spectroscopy to Optimise Food Product Mixing

Angela Barone[a], Jarka Glassey[a*], Gary Montague[b]

[a]School of Engineering, Newcastle University, Newcastle upon Tyne, NE1 7RU, UK

[b]School of Science, Engineering and Design, Teesside University, Middlesbrough, TS1 3BX, UK

Abstract

This paper advances the use of in-situ Near-Infrared (NIR) spectroscopy as the basis for an in-line control system to optimise mixing time of food powder blends. A non-contact NIR fibre-optic probe installed in a conical screw mixer was used to scan three powder mixtures characterised by different particle size distribution and component distribution. The current state of the art is extended by comparing Conformity Index and Standard deviation of the Moving Block Standard Deviation (MBSD), establishing the optimal pre-treatment combination and investigating the effects of the mixture properties on the results. Products with a broad particle size distribution were more accurately represented using derivatives rather than SNV and Detrending, while products with a broad component distribution showed good results with all pre-treatments.

This study evaluated the effect of data pre-treatments on mixing time for different physical properties of powder blends and provided a general guidance on the most appropriate pre-treatment.

Keywords

Powder mixing, Near-infrared, food, quality control, spectroscopy

* Corresponding Author

1 Introduction

Food manufacture is subject to many safety and quality regulations in order to reassure the consumer that the product is free from any unwanted substance and provide customers with a consistent quality. Quality inspection protocols need to be in place to ensure confidence that products leaving the plant fall within safety regulations and customer specification. Effective quality control is thus a preeminent consideration in the food industry in that it ensures customer satisfaction and safety are achieved as far as possible.

The attention of this study will be directed towards powder blending processes which are very common in the food industries (Cullen, 2009). Mixing time has to date been typically based on experimental experience and generally extended far beyond the time when full homogeneity was indicated to accommodate natural variability and perceived risk. Off-line testing by taking samples from a vessel and then performing a destructive analysis have been the most common option to assess the product quality, however this method is time-consuming and often error-prone. Samples are not necessarily representative of the entire batch and the insertion of the thief probe disturbs the powder bed, so compromising the sampling and resulting in an inaccurate measurement. Segregation issues in the sample compartment may arise if the particle size distribution of the components is wide (El-Hagrasy et al., 2001). In addition, results are typically obtained after the production is ended, so not providing a prompt feedback in the case of deviation. A detailed literature review of powder mixing and standard sampling procedures can be found in the work of Muzzio, Goodridge et al. (2003).

Recent studies focussed on the in-line monitoring of food powder blending processes and in particular on the evaluation of blend uniformity. Process Analytical Technology (PAT) comprises a series of tools for designing and controlling manufacturing processes online and has been employed by several types of industries aiming at ensuring the final product quality and increasing the efficiency.The recent developments and main challenges to adopting PAT in the food industry have been discussed (Cullen et al., 2014).

Near-Infrared spectroscopy (NIR) is the most popular PAT system adopted as an inline method to monitor the powder blending process. Radiation in the NIR frequency range hits the sample and

provides spectra containing information on molecular absorption of overtones and combination bands (Burns and Ciurczak, 2008). These spectra used to be difficult to interpret since a single band may result from several combinations of fundamental and overtone vibrations, but progress in chemometric tools now makes it easier to decode spectra, relate them to sample properties and recognise scatter effects (Reich, 2005). The first industrial applications of NIR spectroscopy were in the 1960s with the work of Norris and Hart (1963) who measured the moisture of agricultural products. From then on, NIR spectroscopy gained importance in industry especially because it allows monitoring and controlling the process in real time, without being invasive.

Mixing time has been assessed for different blending processes: for instance, NIR probes were applied to a modified V- blender (Sekulic et al., 1996), a Nauta mixer (Berntsson et al., 2002) and a lab-scale blender (Blanco et al., 2002). Further applications can be found in the work of Blanco, Cueva-Mestanza et al. (2012) which provided a good review of blending time assessment and a detailed comparison of the different methods and pre-treatments. Given the great success of NIR in estimating the end time of powder blending, this technique was also employed to monitor and determine the end time of other processes. For instance, NIR was applied to a fluid bed granulation (Alcalà et al., 2010), a red peony root extraction (Wu et al., 2012) and a pan tablet coating process (Möltgen et al., 2012). All these studies proved the feasibility of NIR as an inline instrument to monitor the production and optimise the mixing time. Other studies focussed their attention on the optimisation of the parameters to obtain more accurate results. It was demonstrated that multiple sampling points provide for accurate and precise estimation of mixing end points (El-Hagrasy et al., 2001, Scheibelhofer et al., 2013). Critical factors affecting powder blending, such as humidity, component concentration, blender speed, particle size and powder density were identified (El-Hagrasy et al., 2005). The effects of temperature and moisture content on the dehydration behaviour of different materials were studied (Räsänen et al., 2003).

With this study the aim is to advance the field by establishing the optimal pre-treatment combination and investigating the effects of the mixture physical properties on the results. Specifically, the main purpose is to evaluate the influence of the distributions of the components and the particle size on the results and on the choice of the pre-treatment. The study subsequently also

aims to optimise the mixing time of food powder blends. Analyses were repeated using two different methods in order to verify the assumption that the effects of the physical properties and of the pre-treatments were not depending on the algorithm employed. Homogeneity analyses in this way will be tailored depending on the specific product and its properties. This will increase the accuracy of the analyses and provide a more reliable result. This paper thus describes how with deep process understanding, sophisticated measurement and appropriate data pre-treatment, the approach to assessing powder homogeneity in food mixing using NIR can be further improved.

2 Materials and methods

2.1 Materials

The formulation of the materials used in this study cannot be revealed due to industrial confidentiality reasons, but all the information required to place the research advances outlined in context and to underpin the justifications are described.

Bread and confectionery powder mixtures aimed at the bakery market were analysed in this study; the main components were flour, sugar, gluten and salt. Three different products were taken into consideration:

- Product A: a blend with a narrow particle size distribution and more than one main component;
- Product B: a blend with a narrow particle size distribution and one main component that counts for more than 90% of the mass;
- Product C: a blend with a broad particle size distribution and more than one main component.

Figure 1 shows histograms with particle sizes of Product A and Product C and provides the mass percentage for each component. Product A component dimensions range from 0.1 mm to 0.5 mm and thus the size distribution is narrow. However, Product C has a broad particle size distribution; from a minimum value of 0.09 mm to a maximum of 10 mm. Dimensions thus vary by more than two magnitudes. Mass percentages of Product B components are 93.22% , 5.08% and 1.71%.

2.2 Instrumentation

The experiments were performed using two conical screw mixers, each one equipped with a diffuse reflectance fibre-optic probe. The fibre optic probe was installed on a side of the vessels at about 1.5 m from the bottom, which resulted to be the best physical location. The probe position is a compromise between being sufficiently low in the vessel so as to scan blends at the starting of the material loading phase, but not too low to prohibit installation welding requirements which need to be undertaken from the inside of the vessel. Both blenders have a nominal capacity of 4000 l, are 3.52 m high and probes are installed on a side of the vessel at about 1.5 m from the bottom. The screw orbit arm rotates with a speed of 1.2 rpm, while the screw itself rotates at 70 rpm and at a distance of 5 mm from the vessel side, so guaranteeing the glass probe cleanliness and avoiding powder remaining stuck on it. Figure 2 shows the configuration of the conical screw mixer and how the NIR probe is connected to the blender.

The fibre optic NIR heads contain two tungsten light sources which illuminate the sample. Scattered light is collected by a thermo-electrically cooled InGaAs detector and guided via a 60 m long fibre optic cable to the Bruker Matrix-F FT-NIR spectrometer. The probe outer diameter is 12.5 cm while the nominal sampling diameter is 10 mm, which corresponds to a measurement area of 0.78 cm^2. Spectral data were collected using OPUS software version 7.0 and analysed with Matlab version R2014a. The spectral resolution was 16 cm^{-1} and frequency region ranged from 10000 cm^{-1} to 4600 cm^{-1} (1000 nm – 2174 nm), resulting in 700 data points per sample. The sampling frequency was set to 20 scans per spectrum and the total time between each spectrum was approximately 31 seconds.

2.3 Methods

Spectra were collected continuously during the whole production time from the point of loading the first ingredient until the process was stopped. The fundamental assumption of the approach is that, when the spectra are consistent and multiple spectral samples overlap each other, homogeneity has been achieved. To support this assumption, off-line NIR probe tests were undertaken considering known well-mixed ingredients, where the formulation was changed to test sensitivity, confirming that

concentration changes were apparent in the NIR signal. In addition, samples of the batches monitored were also test baked and they all performed as expected, proving that their homogeneity levels were sufficient to meet the product specifications. However, given that spectra are subject to noise, data first need to be pre-treated before the analysis. Two methods were investigated to establish spectra overlap: "Conformity Index" and "Standard deviation of the Moving Block Standard Deviation (MBSD)".

2.3.1 Spectral pre-processing

When dealing with solid samples, the data collected is largely influenced by light scattering: the Near-Infrared light beam when hitting the powder sample is partially deflected by the solid particles causing differences in the effective path length that in turn lead to significant variations in spectra. Scattering effects are more likely witnessed in case of uncontrollable physical variations such as non-homogeneous distribution of the particles, changes in refractive index, particle size distribution, sample packing/density variability and sample morphology (Huang et al., 2010). Several pre-treatments algorithms are available to remove scattering and in this study the most frequently applied were considered. Since homogeneity analyses involve spectra belonging to different production phases, and thus to different composition, only pre-treatments employing independent references and isolating each spectrum from the dataset were considered.

Derivatives

Derivatives of spectra are calculated using the Savitzky-Golay algorithm. 1st and 2nd order derivatives are most common: 1st order removes baseline change from spectra, while 2nd order also eliminates linear trends across the spectra (Rinnan et al., 2009). Derivatives are very good at enhancing differences between spectra and differentiate the overlapping signature, but they also increase noise.

Detrending

Detrending subtracts a polynomial fit from the original spectra in order to correct the baseline (Golic and Walsh, 2006). The resulting spectrum is given by:

$$X_{Dt} = X_{orig} - (a_0 + a_1\lambda)$$

where X_{DT} is the spectrum corrected with detrending, X_{orig} is the original spectrum, a_0 and a_1 are polynomial coefficients and λ is the wavelength.

Normalisation

The same weight is given to all the absorbances: each spectrum is in fact normalised to a length of 1 by dividing it by the Euclidian norm (Rinnan et al., 2009).

$$X_{norm} = \frac{X_{orig}}{\sqrt{\Sigma\left(X_{orig}^2\right)}}$$

where X_{norm} is the spectrum normalised and X_{orig} is the original spectrum.

Standard Normal Variate (SNV)

SNV normalises each spectrum to zero mean and unit variance by subtracting the mean of each spectrum and dividing by its standard deviation σ (Rinnan et al., 2009).

$$X_{SNV} = \frac{X_{orig} - X_{mean}}{\sigma}$$

where X_{SNV} is the spectrum corrected with SNV, X_{orig} is the original spectrum, X_{mean} is the average value of the spectrum to be corrected and σ is the standard deviation of the sample spectrum.

2.3.2 Conformity Index

The Conformity Index (CI) was calculated as the difference between every single spectrum acquired and the target spectrum referred to the homogeneous blend; then this difference was weighted by the corresponding standard deviation σ on the respective wavelength.

$$\boldsymbol{CI_i = \frac{spectra\ matrix_{i,j} - \ target\ spectrum}{\sigma_i}}$$

The Conformity Index has been used in previous studies to test the identity of the product and check potential unconformities (Bodson et al., 2006, Pestieau et al., 2014). The result is a second matrix where every column represents the difference between a single spectrum and the target one; for every

column the maximum values were calculated in order to create the vector describing the homogeneity trend.

Target spectrum has to be representative of the finished product, hence spectra were collected at the production end of multiple batches of the same powder blend and then averaged. All batches were manufactured following the same production instructions: the mixing screw was activated at the process start and raw materials are manually loaded into the vessel by operators while the screw is rotating. Then when the loading phase is over, the screw is left rotating for a time which is specific for every product and based on experience and is considerably in excess of what is required to attain complete mixing. The number of the spectra included varied depending on the production frequency and thus on the data availability. 50 spectra were used for Product A, 40 spectra for Product B and 100 spectra for Product C.

2.3.3 Standard deviation of Moving Block Standard Deviation (MBSD)

The standard deviation was calculated in both the wavelength and time domains. Initially the standard deviation was calculated for every group of three consecutive spectra in the wavelength domain, so forming the Moving Block Standard Deviation (MBSD) matrix. The standard deviation was then calculated for each individual wavelength and the final vector obtained showed how spectra changed over time (Sekulic et al., 1996).

The main advantage of MBSD is that it is calibration-free and thus it does not require a reference spectrum. Hence analyses can be performed with no need of previous studies (Momose et al., 2011). A block of three spectra in MBSD was found to be the optimal size after investigating how the block dimension could impact on the results.

3 Results and discussion

In all the experiments the change of spectra over time was observed, eventually converging to the steady state spectrum (see the example in Figure 3). The green spectra represent the beginning of the production, when the blend was still under the level of the probe. The characteristic flat shape is due

to the fact that what is scanned in this phase is only the air present in the mixer. As air does not contain any organic component, no relevant peaks can be observed in its spectra, therefore giving a flat shape. As soon as the probe starts getting covered by the powder mixture, the spectra begin to show a few peaks. This is represented by the blue spectra. The position of the peaks is related to the different molecular groups, while the height of peaks depends on the concentration. Blue spectra are shown to change over time indicating the composition is changing. In fact, during the process different ingredients are added and blends are continuously mixed, leading to different powders being scanned by the NIR probe. Spectra are seen to start to overlap after a certain time, as illustrated by the red spectra. Since each sample of a given composition and concentration is uniquely identified by a spectrum, the overlap demonstrates that samples of equal composition and concentration are being scanned. As the powder is still being mixed by the screw, scans resulting in a near identical signal are only possible if all the powder inside the mixer has the same concentration, thus indicating the blend is homogeneous. Mixing time is therefore determined by the time it takes for the spectra to overlap with each other and a steady state fully mixed spectrum is reached. Both methods, “Conformity Index” and “Standard deviation of MBSD”, were applied to estimate this mixing time. Initially the influence of pre-treatments on the calculation of mixing time was studied; subsequently it was assessed whether the results of these homogeneity studies was affected by the physical properties of the powder blend. The effect of component distribution was evaluated comparing results obtained for Product A and B, while particle size distribution was studied by investigating the different effects on Product A and C.

3.1 Conformity Index

The entire blend run was analysed employing different pre-processing techniques. Analyses were repeated for 20 different batches to verify the reproducibility of the results. Blending profiles of Conformity Index for Product A are shown in Figure 4.

Variations in profiles were observed when using pre-treatments, demonstrating the important role of pre-processing algorithms in the estimation of mixing time. However, for all the experiments, an overall qualitative behaviour was observed for four phases:

1) *1st stationary phase*: the profile is stable over time and its highest value is recorded. Powder is still under the level of the probe and NIR is scanning only air which is very different from the final powder blend due to both composition and state of matter. When loading the ingredients inside the vessel, powder starts to disperse in the air phase, but not enough to determine any variation in composition. The green spectra shown in Figure 3 represent this phase;
2) *Decreasing phase*: the CI suddenly decreases due to the powder approaching the probe level. NIR starts scanning a powder mixture which is closer in composition and state of matter to the final powder blend compared to the air phase. Referring to Figure 3, this phase illustrates the passage from green to blue spectra;
3) *Oscillations*: the profile changes over time as a consequence of the variation in composition during the production process. Spectra being scanned in this phase might present different peaks due to new ingredients loaded into the vessel. The continuously rotating screw moves the powder through the whole mixer, causing changes in composition even when loading of ingredients is completed. Blue spectra shifting over time in Figure 3 describe the phenomenon of oscillations;
4) *2nd stationary phase*: the profile finally approaches the zero value and remains stable over time. When spectral differences are no longer recorded, the scanned mixture has the same composition and concentration of the ideal mixture. The stationary character of the results means the blend composition is stable over time, hence it can be assumed that full homogeneity is reached. Red spectra overlapping to each other in Figure 3 represent the 2nd stationary phase.

Mixing time is thus given by the starting point of the 2nd stationary phase, the sensitivity of detection of which may change depending on the pre-treatment chosen. It is therefore of vital importance to understand the effect of the different pre-treatments.

As can be seen in Figure 4, a plot of raw data (a) differs enormously from the ones obtained following any pre-treatment: there is a peak in the 1st stationary phase and decreasing phase is soon followed by 2nd stationary phase (starting at minute 4 in Figure 4(a)). Since it is unlikely that the blend reaches the homogeneity soon after the powder mixture reaches the level of the probe, it is concluded that raw data do not describe the process satisfactorily. Scattering effects in fact dominate when the

blend is under the level of the probe as a relatively small quantity of powder particles is dispersed in the gas phase and NIR light deviates from the original path length. All pre-processing algorithms studied (first and second derivatives, normalisation, SNV, and detrending) contribute to removing scattering effects and to make the homogeneity starting point more distinct (Figure 4 b-f).

In order to investigate the effect of component distribution on choosing the right pre-treatment, the same study was performed on Product B, which presents a very small variability given that more than 90% of the product is represented by the same component. The Conformity Index was evaluated for 18 different batches of Product B. Figure 5 presents the blending run profiles obtained for Product B. None of the pre-treatment methods studied were able to reliably estimate mixing time due to the oscillation phase not being accentuated sufficiently and thus being confused with the 2nd stationary phase. Changes in composition are not easy to detect as a consequence of the reduced component distribution of the product. The Conformity Index was shown not to be a suitable method for measuring mixing time of blends with concentrations of a single component higher than 90% given the lack of variability in the mixture.

In order to study the effect of particle size distribution on the pre-treatment choice, Conformity Index analyses were performed on Product C. Calculations were repeated for 29 different batches of Product C and an example of the results obtained is shown in Figure 6. The first notable difference compared with profiles of Product A is the presence of high peaks during the oscillation phase at 11 minutes. Before this all the ingredients in the vessel had a similar nature and a similar particle size. Soon after the introduction in the mixer of particulates almost 100 times larger than the other components, the blend became more heterogeneous presenting parts of only fine powder and parts of only particulate. Peaks at 11 minutes represent the variation when scanning the different parts of the blend (fine powder and particulate). After these few peaks, the oscillation phase returns to that exhibited prior to the addition due to the continuous movement of the screw acting to mix all the ingredients (redistributed fine powder and particulate making the mixture homogeneous). Pre-treatments such as SNV and Detrending show slight oscillations in the 2nd stationary phase, making the homogeneity starting point less clear. Better results were achieved by derivatives, especially second derivative, as the 2nd stationary phase was flatter and it was more evident when the oscillation

283 phase ends. Due to the greater variability introduced by the increase in particle size distribution, the
284 system was more heterogeneous and differences in spectra were enhanced. Pre-processing such as
285 SNV accentuated these differences even when the mixture was homogeneous: the stationary phase
286 was more oscillatory and it was more difficult to clearly assess mixing time. Derivatives on the other
287 hand were less sensitive to these variations and still clearly showed the start of the 2nd stationary
288 phase, so defining the mixing time. Since Product C is characterised by a broad particle distribution,
289 in order to assess its homogeneity, the distribution of particle sizes cannot be ignored. Techniques
290 such as SNV and Detrending were actually born to reduce particle size effects (Zeaiter et al., 2005)
291 hence they might be less suitable to analyse products with broad particle distribution. Derivatives, on
292 the other hand, retain the effects of particle size contained in a NIR spectrum. These results were
293 confirmed by a previous study determining the particle size distribution of a solid product: calibration
294 models built by pre-treating data with SNV achieved higher errors than by pre-treating data with
295 second derivative (Blanco and Peguero, 2008). Table 1 shows mixing time results for Product A and
296 Product C obtained using different pre-treatments.
297 Results obtained analysing blending run profiles using different pre-treatment techniques
298 demonstrated the importance of data pre-processing in the Conformity Index studies. In addition,
299 considering different product categories demonstrated how the choice of pre-treatment actually
300 depends on the properties of the powder blend. In order to set up a general method valid for every
301 product, the best option is to adopt a combination of pre-treatments, rather than relying on just one
302 technique, in order to obtain all the advantages provided by each algorithm. Normalisation was taken
303 into consideration as for all the experiments it proved to be best for the removal of initial scattering
304 effects which cause unwanted peaks after the 1st stationary phase. On the other hand it also flattens
305 oscillations making mixing time less evident, so other pre-treatments able to accentuate differences
306 need to be used together with Normalisation. Two combinations were studied: Normalisation + SNV
307 + Detrending and Normalisation + 2nd derivative. Results are presented in Figure 7. Product A mixing
308 time can be clearly estimated using both combinations (Figure 7 (a), (b)), but homogeneity of Product
309 B cannot be analysed properly by any of the combinations employed (Figure 7 (c), (d)). The blend
310 appears homogeneous as soon as the powder reaches the probe (minute 12), due to the extreme

component distribution. Product C mixing time can be estimated accurately using Normalisation + derivative, but not by Normalisation + SNV + Detrending (Figure 7 (e), (f)). The large variation in the particle size distribution of Product C is in fact responsible for the increase in variability, and SNV and Detrending accentuate these differences excessively, causing oscillations also in the 2nd stationary phase. Table 2 provides mixing time results for Product A, B and C obtained using pre-treatments combinations of Normalisation+SNV+Detrending and Normalisation+1st derivative.

When analysing and test baking production samples, the time provided by Normalisation+SNV+Detrending and Normalisation+1st derivative for Product A (33.25 minutes) was estimated to be the mixing time of the batch analysed, which resulted in saving 26% of the total time the product was mixed (45 minutes). While for Product C, time provided by Normalisation+1st derivative (46.67 minutes) was estimated to be the mixing time of the batch analysed, so saving about 22% of the total time the product was mixed (60 minutes).

Normalisation + SNV + Detrending gives all the benefits provided by these three techniques: initial scattering is removed, the oscillation phase is emphasised and the homogeneity starting point is clearly detectable. This combination can be generally used for products with average or narrow component distribution, but not for products with a single component concentration higher than 90%. For this kind of material, represented here by Product B, the Conformity Index cannot be used reliably to estimate the mixing time. Concerning particle size distribution, the preference is to employ Normalisation + derivative as differences would be accentuated too much by SNV-Detrending due to the high variability involved in these products.

3.2 Standard deviation of Moving Block Standard Deviation (MBSD)

Following analysis using the CI, the entire blend run was re-analysed with MBSD and different pre-processing techniques in order to evaluate their effects. The same batches used to test the validity of Conformity Index were further analysed using MBSD. Again the plots can be generally divided in four parts, looking very similar to those seen for the Conformity Index. The only difference is given by the high peak replacing the decreasing phase: standard deviation comes through a big rise due to the significant change in composition recorded when powder approaches the probe level. Mixing

time, as with "Conformity Index" analysis, corresponds to the starting point of the 2nd stationary phase.

Products A, B and C were analysed and compared in order to investigate the effect of component distribution and particle size distribution when pre-treatment approaches are applied with the Standard deviation of MBSD. Blending profiles of Standard deviation of MBSD for Products A, B and C using the pre-treatment combinations Normalisation + SNV + Detrending and Normalisation + 1st derivative are compared in Figure 8.

The same pre-treatment effects as found for the CI were found with MBSD, despite the two methods focusing on different aspects. Product A was well described by both Normalisation + SNV + Detrending and Normalisation+1st derivative as can be seen by comparing the plots in Figure 8 (a) and (b): same mixing time was estimated. Product B could not be analysed employing any of the pre-treatments or their combinations (Figure 8 (c) and (d)), and Product C could only be analysed using Normalisation + derivative (Figure 8 (e) and (f)).

3.3 Control program

A program was developed to automate the homogeneity assessment into the factory control systems in order to provide on-line indications of the mixing extent for the production process and ultimately move to in-line control. A model for Conformity Index was built using the specific application in OPUS software; for every product the target spectra were loaded and the best pre-treatment combination and frequency range were specified. A lower limit of maximum Conformity Index combined with a time under the limit criterion was used to indicate homogeneity. A script was written using a text-based programming language in OPUS: the program includes one main program and a sub-program that is called by the main program to calculate the time spent below the lower limit of CI. The control program starts when the loading phase is over: the main script is initially run and spectra are continuously collected during the mixing phase. For every scan, CI is calculated using the model previously built and a check is made to ascertain whether the value is below the lower limit previously set. One possible practical issue arises due to the oscillatory nature of the signal as a consequence of mixing before homogeneity is achieved. As homogeneity approaches, the signal may

fall and rise repeatedly around the threshold. To avoid this issue, the program continues running until consecutive values of CI under the lower limit are obtained for a specified time window. If the CI falls below the limit and subsequently rises above the limit before the time limit criterion is satisfied the blend cannot be considered homogeneous and the time counter is reset. This time was set to a value of 5 minutes. This was determined through experience and behaviour of the historical batches. Once the signal remains below the threshold for the specified time, in this case 5 minutes, the program is stopped and a message is displayed on the screen indicating that the blend is homogeneous and the process can be stopped.

A possible situation could arise if the signal is noisy in that it may repeatedly fail to reach the time criterion due to signal noise. For practical operational reasons, a limit is set based on existing over cautious settings and, if 15 minutes has passed, a message is displayed saying that homogeneity cannot be established.

Applying this control method to the data of the batches previously produced, it was evaluated that up to 15 minutes of unnecessary blending and up to a third of the total batch production time can be saved. This can lead to an increase in the productivity of about 33% with consequent benefits on the profits.

4. Conclusions

The Conformity Index and Standard deviation of Moving Block Standard Deviation (MBSD) both demonstrated their capability to determine homogeneity and they indicated the same mixing time. Blending run profiles are quite different, but both can be divided in four parts: the last part being a 2nd stationary phase whose beginning indicates the homogeneity starting point.

Raw data were not able to accurately determine the mixing time due to scattering effects obscuring important information. Blending profiles generally improved by pre-treating data, in particular derivatives were preferred for products with broad particle size distribution, as oscillations were less enhanced and starting of 2nd stationary phase was more evident. Derivatives indeed retain the effects of particle size contained in the spectra which need to be considered to assess the homogeneity of products with broad particle size distribution. Neither the Conformity Index nor the Standard

deviation of MBSD were able to provide satisfactory estimates of the mixing time for products characterised by a very narrow component distribution. These products show a high concentration of one of the components (>90%) and none of the pre-treatment methods used nor their combinations appeared to improve the mixing time predictions. Other methods need to be found to assess homogeneity in products with a very narrow component distribution.

The study was performed using one type of mixer and three materials and it provides a general guidance on the choice of pre-treatment based on particle size distribution and component distribution of the material. Employing a different blender will surely affect the mixing time results, but should not modify the target spectrum hence differences in mixing time evaluation process for the same material should not be relevant and same pre-treatment should be applied. On the other hand, the use of a different powder blend requires a prior investigation of the best pre-treatment before determining the mixing time since particle size distribution and component distribution do not fully describe the material. The amount of time and effort required to optimise pre-treatment mainly depends on the data available, hence on the production frequency of the material under investigation. Mixing time evaluation of products frequently manufactured will require a shorter time and a smaller level of effort. The cost of operation will increase in an initial phase mainly due to more resources needed to perform the analysis. However, after the model assessing mixing time has been built, this would only require maintenance and operation costs will decrease. As the method is deployed in the factory, experience will determine the breakeven point balancing increased initial resource against long term mixing time savings. Such financial considerations are confidential to our collaborating company but suffice to say role out of the technology is ongoing.

This study revealed the still unexplored effects of particle size distribution and component distribution on the choice of the pre-treatment so representing a further step in the evaluation of mixing time using Near-Infrared spectroscopy. Awareness of these properties and their effects allows optimisation of blending time and helps reducing the risk of under/over-mixing.

Acknowledgements

The authors would like to acknowledge the financial support of UK Engineering and Physical Sciences Research Council under grant EP/G037620/1. The input of the industrial partner in the financial support of Angela Barone and the undertaking of on-site trials is also gratefully acknowledged.

References

ALCALÀ, M., BLANCO, M., BAUTISTA, M. & GONZÁLEZ, J. M. 2010. On-line monitoring of a granulation process by NIR spectroscopy. *Journal of Pharmaceutical Sciences,* 99**,** 336-345.

BERNTSSON, O., DANIELSSON, L.-G., LAGERHOLM, B. & FOLESTAD, S. 2002. Quantitative in-line monitoring of powder blending by near infrared reflection spectroscopy. *Powder Technology,* 123**,** 185–193.

BLANCO, M., CUEVA-MESTANZA, R. & CRUZ, J. 2012. Critical evaluation of methods for end-point determination in pharmaceutical blending processes. *Analytical Methods,* 4**,** 2694-2703.

BLANCO, M., GOZÁLEZ BAÑÓ, R. & BERTRAN, E. 2002. Monitoring powder blending in pharmaceutical processes by use of near infrared spectroscopy. *Talanta,* 56**,** 203–212.

BLANCO, M. & PEGUERO, A. 2008. An expeditious method for determining particle size distribution by near infrared spectroscopy: Comparison of PLS2 and ANN models. *Talanta,* 77**,** 647-651.

BODSON, C., DEWÉ, W., HUBERT, P. & DELATTRE, L. 2006. Comparison of FT-NIR transmission and UV–vis spectrophotometry to follow the mixing kinetics and to assay low-dose tablets containing riboflavin. *Journal of Pharmaceutical and Biomedical Analysis,* 41**,** 783–790.

BURNS, D. A. & CIURCZAK, E. W. 2008. *Handbook of Near-Infrared Analysis, Second Edition*.

CULLEN, P. J. 2009. *Food Mixing: Principles and Applications*, John Wiley & Sons.

CULLEN, P. J., O'DONNELL, C. P. & FAGAN, C. C. 2014. Benefits and Challenges of Adopting PAT for the Food Industry. *Process Analytical Technology for the Food Industry.* New York: Springer.

EL-HAGRASY, A. S., MORRIS, H. R., D'AMICO, F., A. LODDER, R. & DRENNEN III, J. K. 2001. Near-infrared spectroscopy and imaging for the monitoring of powder blend homogeneity. *Journal of Pharmaceutical Sciences,* 90**,** 1298-1307.

EL-HAGRASY, A. S., D'AMICO, F. & DRENNEN, J. K. 2005. A Process Analytical Technology approach to near-infrared process control of pharmaceutical powder blending. Part I: D-

optimal design for characterization of powder mixing and preliminary spectral data evaluation. *Journal of Pharmaceutical Sciences,* 95**,** 392-406.

GOLIC, M. & WALSH, K. B. 2006. Robustness of calibration models based on near infrared spectroscopy for the in-line grading of stonefruit for total soluble solids content. *Analytica Chimica Acta,* 555**,** 286–291.

HUANG, J., ROMERO-TORRES, S. & MOSHGBAR, M. 2010. Practical Considerations in Data Pre-treatment for NIR and Raman Spectroscopy. *American Pharmaceutical Review,* 13**,** 116.

MÖLTGEN, C.-V., PUCHERT, T., MENEZES, J. C., LOCHMANN, D. & REICH, G. 2012. A novel in-line NIR spectroscopy application for the monitoring of tablet film coating in an industrial scale process. *Talanta,* 92**,** 26–37.

MOMOSE, W., IMAI, K., YOKOTA, S., YONEMOCHI, E. & TERADA, K. 2011. Process analytical technology applied for end-point detection of pharmaceutical blending by combining two calibration-free methods: Simultaneously monitoring specific near-infrared peak intensity and moving block standard deviation. *Powder Technology,* 210**,** 122-131.

MUZZIO, F. J., GOODRIDGE, C. L., ALEXANDER, A., ARRATIA, P., YANG, H., SUDAH, O. & MERGEN, G. 2003. Sampling and characterization of pharmaceutical powders and granular blends. *International Journal of Pharmaceutics,* 250**,** 51-64.

NORRIS, K. H. & HART, J. R. 1963. Proceedings of the 1963 International Symposium on Humidity and Moisture. 4**,** 19–25.

PESTIEAU, A., KRIER, F., THOORENS, G., DUPONT, A., CHAVEZ, P. F., ZIEMONS, E., HUBERT, P. & EVRARD, B. 2014. Towards a real time release approach for manufacturing tablets using NIR spectroscopy. *Journal of Pharmaceutical and Biomedical Analysis,* 98**,** 60–67.

RÄSÄNEN, E., RANTANEN, J., MANNERMAA, J.-P., YLIRUUSI, J. & VUORELA, H. 2003. Dehydration studies using a novel multichamber microscale fluid bed dryer with in-line near-infrared measurement. *Journal of Pharmaceutical Sciences,* 92**,** 2074-2081.

REICH, G. 2005. Near-infrared spectroscopy and imaging: Basic principles and pharmaceutical applications. *Advanced Drug Delivery Reviews,* 57**,** 1109-1143.

478 RINNAN, Å., VAN DEN BERG, F. & BALLING ENGELSEN, S. 2009. Review of the most
479 common pre-processing techniques for near-infrared spectra. *TrAC Trends in Analytical*
480 *Chemistry*, 28**,** 1201–1222.
481 SCHEIBELHOFER, O., BALAK, N., WAHL, P. R., KOLLER, D. M., GLASSER, B. J. &
482 KHINAST, J. G. 2013. Monitoring Blending of Pharmaceutical Powders with Multipoint NIR
483 Spectroscopy *AAPS PharmSciTech*, 14**,** 234–244.
484 SEKULIC, S. S., WARD II, H. W., BRANNEGAN, D. R., STANLEY, E. D., EVANS, C. L.,
485 SCIAVOLINO, S. T., HAILEY, P. A. & ALDRIDGE, P. K. 1996. On-Line Monitoring of
486 Powder Blend Homogeneity by Near-Infrared Spectroscopy. *Analytical chemistry*, 68**,** 509-
487 513.
488 WU, H., JIN, Y., LI, Y., SUN, D., LIU, X. & CHEN, Y. 2012. NIR spectroscopy as a process
489 analytical technology (PAT) tool for on-line and real-time monitoring of an extraction
490 process. 58**,** 109–118.
491 ZEAITER, M., ROGER, J.-M. & BELLON-MAUREL, V. 2005. Robustness of models developed by
492 multivariate calibration. Part II: The influence of pre-processing methods. *TrAC Trends in*
493 *Analytical Chemistry*, 24**,** 437-445.
494

Histograms with particle sizes of Product A (a) and Product C (b). Mass percentages of each components are reported at the bottom of the histogram. Product A components dimensions are similar to each other, while Product C presents a larger variability.

Conical screw mixer configuration. (a) Configuration of the conical screw mixer. (b) Connection of the probe to the blender.

Example of spectra collected during the production phase. Green spectra are recorded when the powder is still under the level of the probe. Blue spectra show powder reaching the level of the probe. Red spectra represent the homogeneous mixture.

Profiles of Conformity Index calculated for Product A. Data were first pre-treated using different pre-processing techniques, and then Conformity Index was calculated. The vertical line represents homogeneity starting point according to the different pre-treatments.

Blending profiles of Conformity Index calculated for Product B. Data were first pre-treated using different pre-processing techniques, and then Conformity Index was calculated.

Blending profiles of Conformity Index calculated for Product C. Data were first pre-treated using different pre-processing techniques, and then CI was calculated. The vertical line represents homogeneity starting point.

Comparison of pre-treatment combinations for Products A, B and C. Data were first pre-treated using Normalisation+SNV+Detrending and Normalisation+2nd derivative, and then Conformity Index was calculated. The vertical line represents the homogeneity starting point. Where the vertical line is missing it was not possible to determine the mixing time.

Comparison of pre-treatment combination for Products A, B and C in Standard Deviation of MBSD analyses. Data were first pre-treated using Normalisation+SNV+Detrending and Normalisation+1st derivative, and then Standard deviation of MBSD was calculated. The vertical line represents homogeneity starting point. Where the vertical line is missing it is because it was not possible to determine mixing time.

Mixing time results for Product A and Product C using different pre-treatments

Mixing time results for Product A, B and C using pre-treatments combinations of Normalisation+SNV+Detrending and Normalisation+1st derivative

	Raw data	1st derivative	2nd derivative	Detrending	Normalisation
Product A [min]	4.08	25.08	30.33	25.08	25.08
Product C [min]	20.42	47.25	41.42	47.83	-

Table 1: Mixing time results for Product A and Product C using different pre-treatments

SNV
27.42
-

	A	B	C
Normalisation+SNV+Detrending	33.83	-	-
Normalisation+1st derivative	33.83	-	46.67

Table 2: Mixing time results for Product A, B and C using pre-treatments combinations of Normalisation+SNV+Detrending and Normalisation+1st derivative

Figure 1 (a)

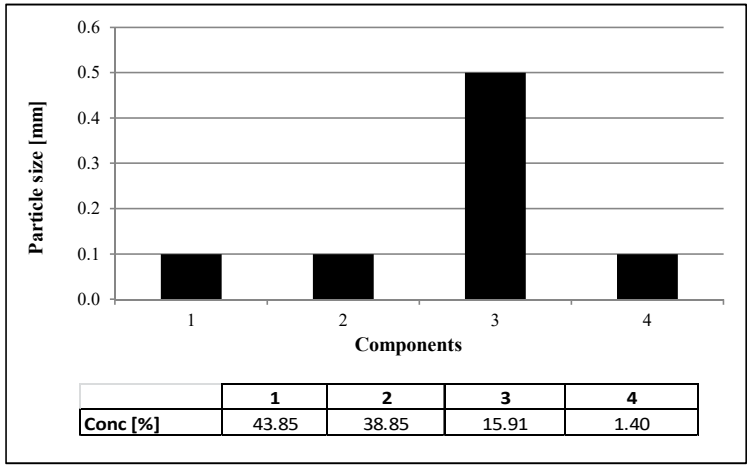

	1	2	3	4
Conc [%]	43.85	38.85	15.91	1.40

Figure 1(b)

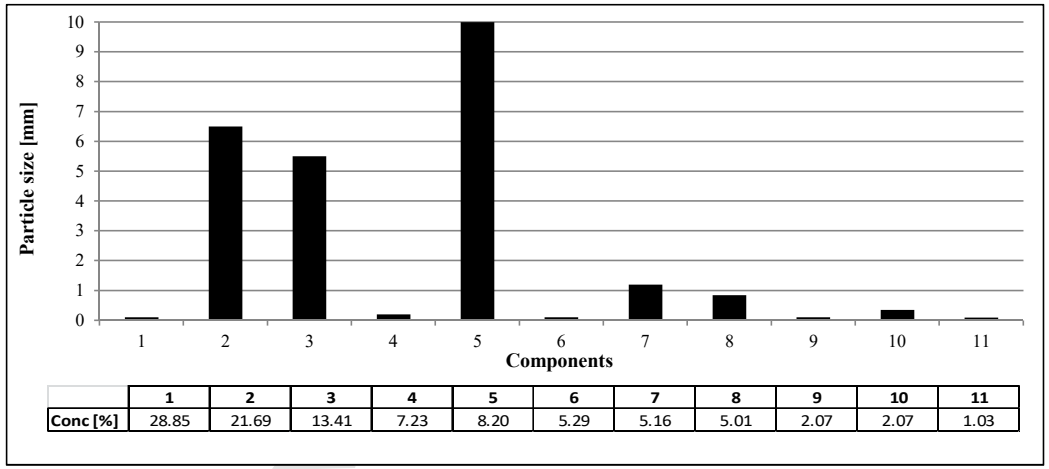

	1	2	3	4	5	6	7	8	9	10	11
Conc [%]	28.85	21.69	13.41	7.23	8.20	5.29	5.16	5.01	2.07	2.07	1.03

Figure 1: Histograms with particle sizes of Product A (a) and Product C (b). Mass percentages of each components are reported at the bottom of the histogram. Product A components dimensions are similar to each other, while Product C presents a larger variability.

Figure 2(a)

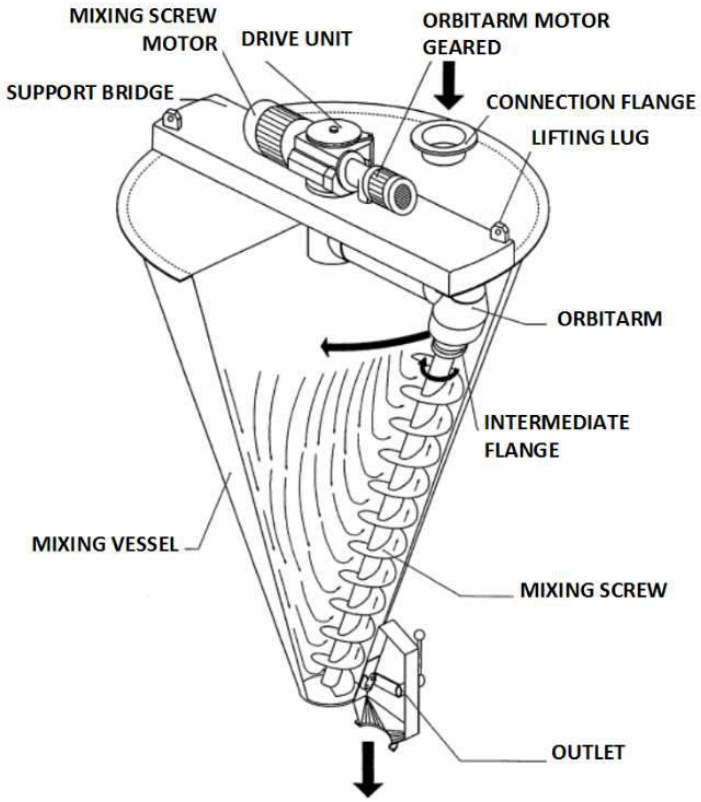

Figure 2(b)

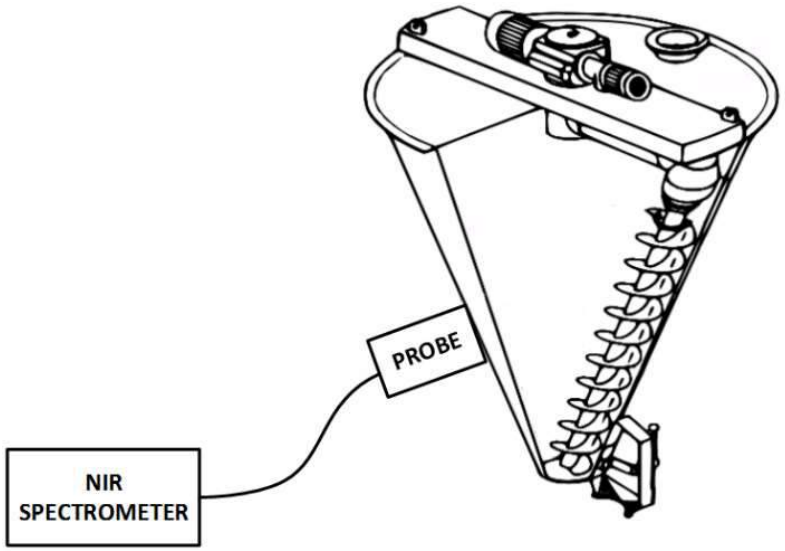

Figure 2: Conical screw mixer configuration. (a) Configuration of the conical screw mixer. (b) Connection of the probe to the blender.

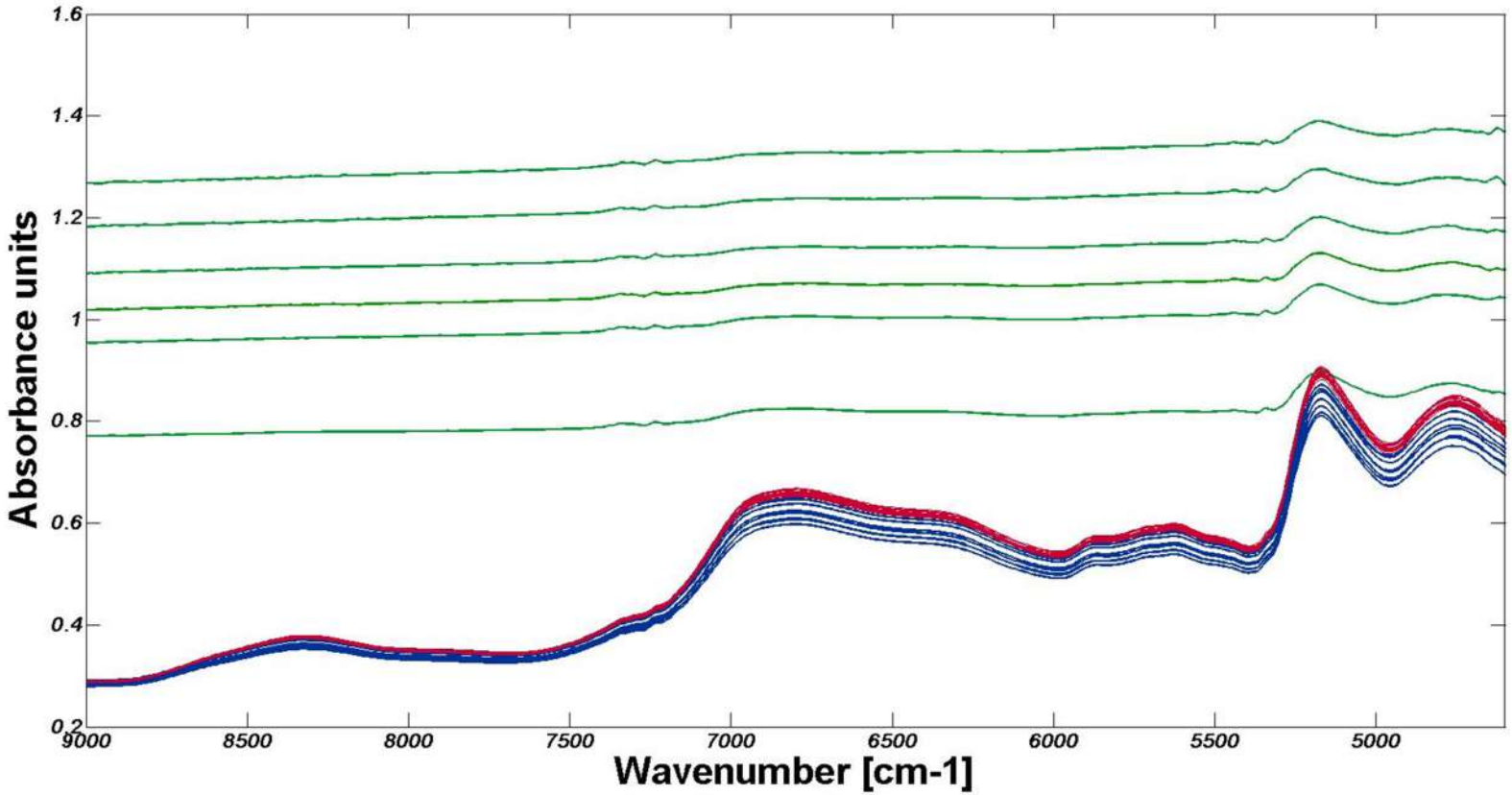

Figure 3: Example of spectra collected during the production phase. Green spectra are recorded when the powder is still under the level of the probe. Blue spectra show powder reaching the level of the probe. Red spectra represent the homogeneous mixture.

Figure 4 (a) Raw data

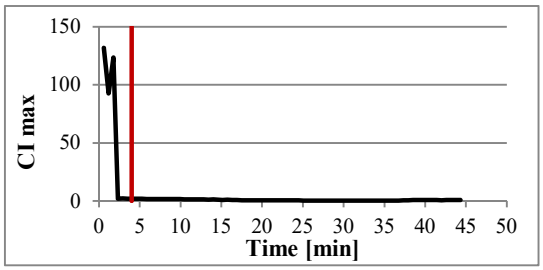

Figure 4 (b) First derivative

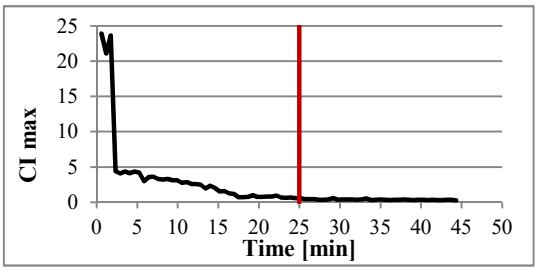

Figure 4 (c) Second derivative

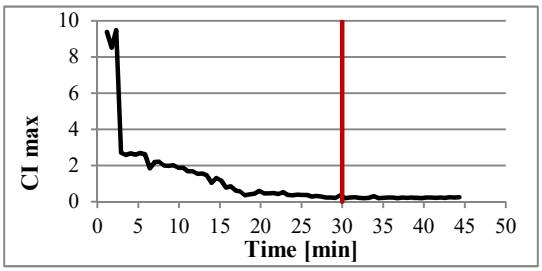

Figure 4 (d) Detrending

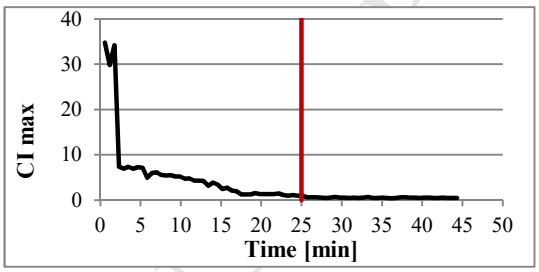

Figure 4 (e) Normalisation

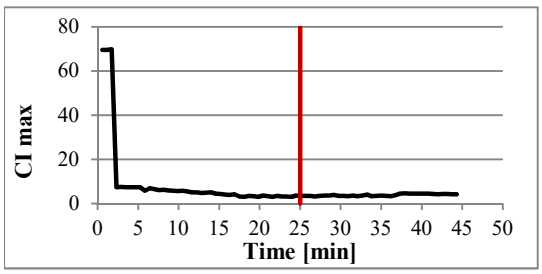

Figure 4 (f) SNV

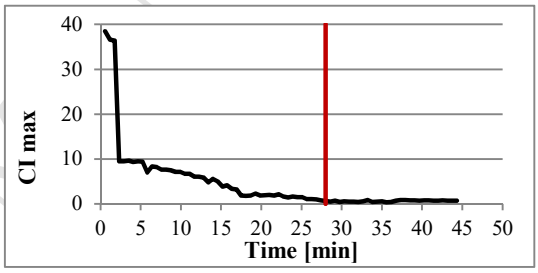

Figure 4: Profiles of Conformity Index calculated for Product A. Data were first pre-treated using different pre-processing techniques, and then Conformity Index was calculated. The vertical line represents homogeneity starting point according to the different pre-treatments.

Figure 5 (a) Raw

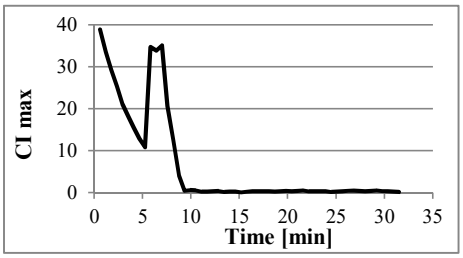

Figure 5 (b) First derivative

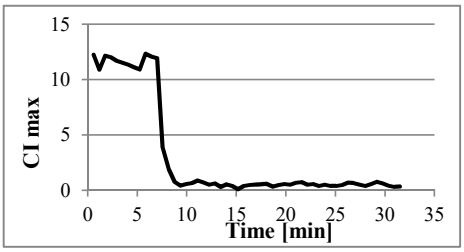

Figure 5 (c) Second derivative

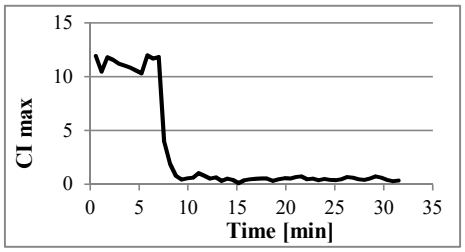

Figure 5 (d) Detrending

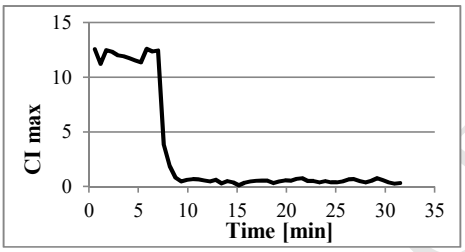

Figure 5 (e) Normalization

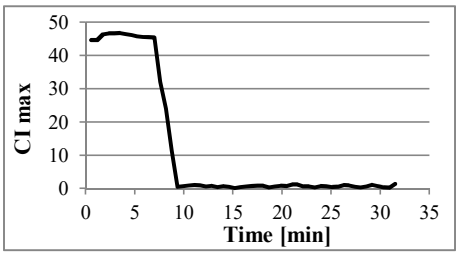

Figure 5 (f) SNV

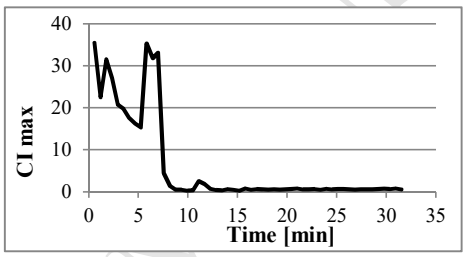

Figure 5: Blending profiles of Conformity Index calculated for Product B. Data were first pre-treated using different pre-processing techniques, and then Conformity Index was calculated.

Figure 6 (a) Raw data

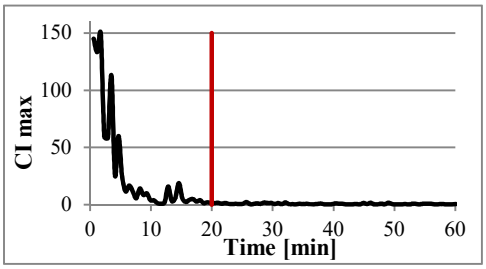

Figure 6 (b) First derivative

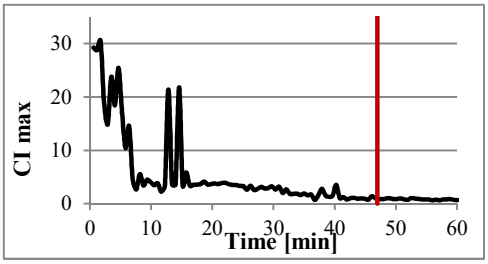

Figure 6 (c) Second derivative

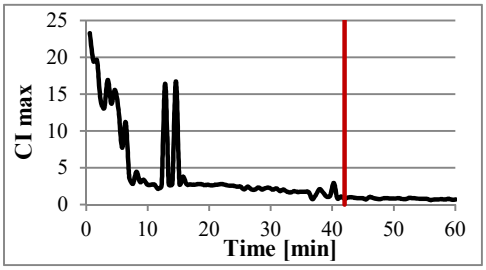

Figure 6 (d) Detrending

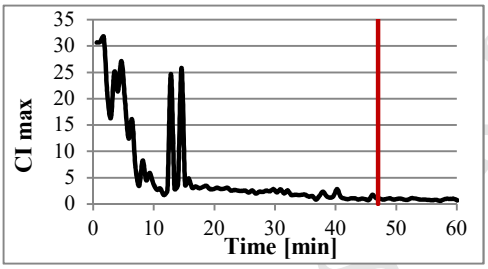

Figure 6 (e) Normalization

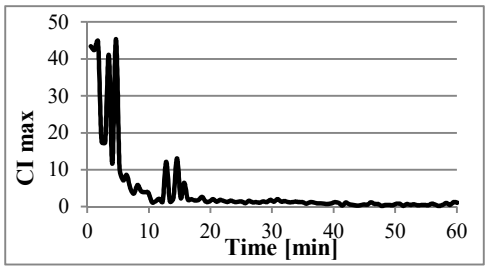

Figure 6 (f) SNV

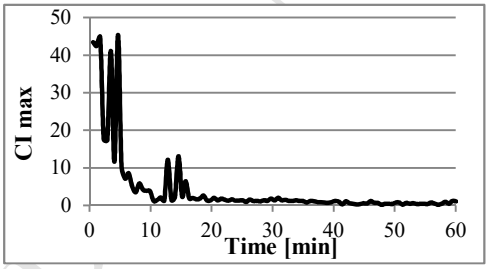

Figure 6: Blending profiles of Conformity Index calculated for Product C. Data were first pre-treated using different pre-processing techniques, and then CI was calculated. The vertical line represents homogeneity starting point.

Figure 7 (a), Product A, Norm-SNV-Dt

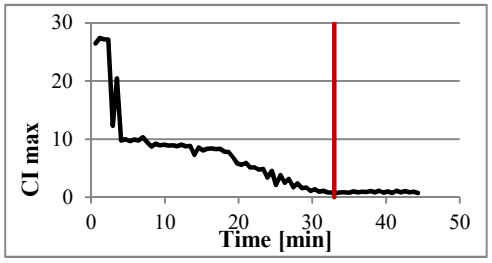

Figure 7 (b), Product A, Norm-First derivative

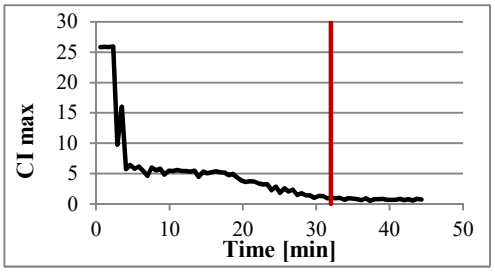

Figure 7 (c), Product B, Norm-SNV-Dt

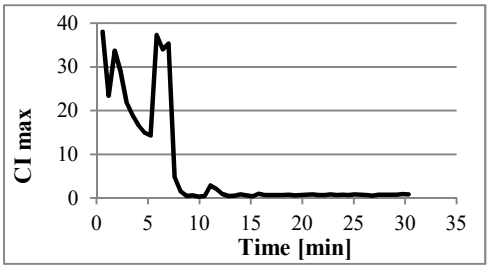

Figure 7 (d), Product B, Norm-First derivative

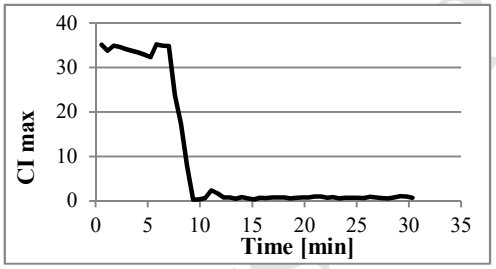

Figure 7 (e), Product C, Norm-SNV-Dt

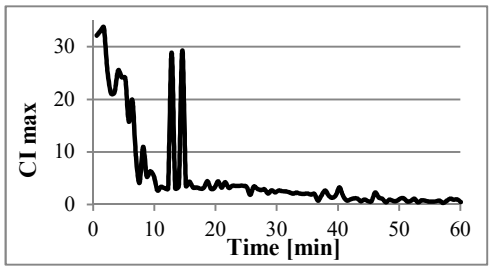

Figure 7 (f), Product C, Norm-First derivative

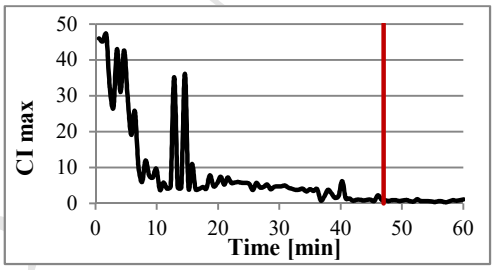

Figure 7: Comparison of pre-treatment combinations for Products A, B and C. Data were first pre-trea using Normalisation+SNV+Detrending and Normalisation+2nd derivative, and then Conformity Index calculated. The vertical line represents the homogeneity starting point. Where the vertical line is missin was not possible to determine the mixing time.

ted
was
g it

Figure 8 (a), Product A, Norm-SNV-Dt

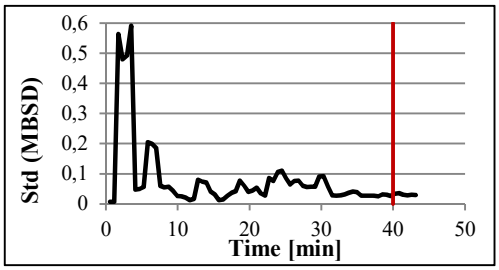

Figure 8 (b), Product A, Norm-First derivative

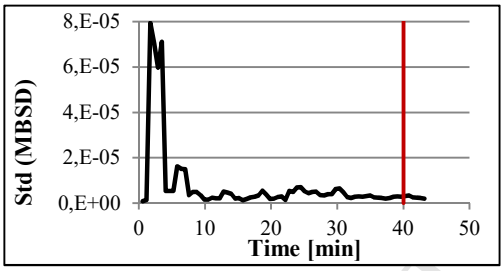

Figure 8 (c), Product B, Norm-SNV-Dt

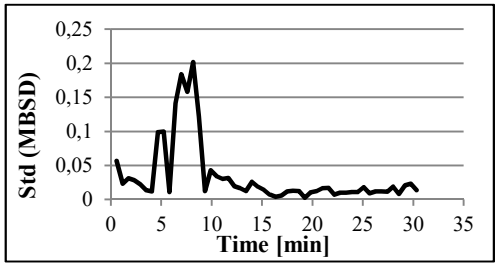

Figure 8 (d), Product B, Norm-First derivative

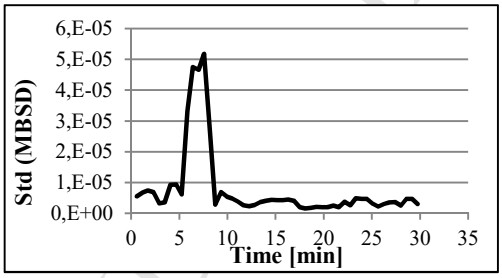

Figure 8 (e), Product C, Norm-SNV-Dt

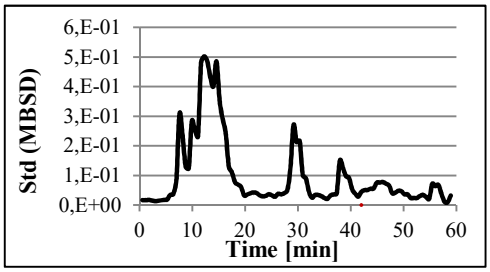

Figure 8 (f), Product C, Norm-First derivative

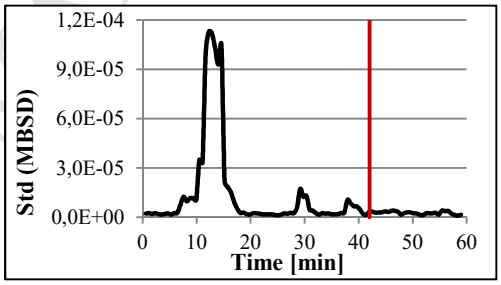

Figure 8: Comparison of pre-treatment combination for Products A, B and C in Standard Deviatic analyses. Data were first pre-treated using Normalisation+SNV+Detrending and Normalisation+1s then Standard deviation of MBSD was calculated. The vertical line represents homogeneity startin the vertical line is missing it was not possible to determine mixing time.

ɔn of MBSD
st derivative, and
ɡ point. Where

Highlights

- Novel approach using Near Infrared spectroscopy to optimise mixing time is proposed
- Particle size and component distribution influence the pre-treatment choice
- Derivatives preferred for products with broad particle size distribution

There is no conflict of interest for any of the authors to be declared.